Mon. Not. R. Astron. Soc. **000**, 000–000 (0000) Printed 17 January 1996 (MN LaTeX style file v1.3)

QSO Clustering - III. Clustering in the LBQS and evolution of the QSO correlation function.

S.M. Croom and T. Shanks
Physics Department, University of Durham, South Road, Durham, DH1 3LE, England.

17 January 1996

ABSTRACT

We present results of clustering analysis for the LBQS, and combine these with results obtained from other QSO surveys including the Durham/AAT UVX sample (Shanks & Boyle 1994). We find a weak signal in the LBQS at small scales, $\bar{\xi}(10\ h^{-1}\ \mathrm{Mpc}) = 1.86 \pm 1.28$ (for $q_\circ = 0.5$). Combined with other samples we find $\bar{\xi}(10) = 0.83 \pm 0.29$, which is consistent with present day galaxy clustering, $\xi \simeq (r/6)^{-1.8}$. To interpret the evolution of QSO clustering we develop a simple biased model of clustering. Using this model and only the high redshift samples our biasing model gives an upper limit on present day QSO clustering of $r_\circ(z=0) = 9.23 \pm 1.11\ h^{-1}$ Mpc (assuming a -1.8 power law), a value which is significantly lower than some previous estimates (Mo & Fang 1993). When we include the observed small amplitude of clustering of $z \sim 0$ AGN (Georgantopoulos & Shanks 1994) in the model fits, we find that the low level of QSO evolution is inconsistent with $\Omega_\circ = 1$, unbiased galaxy, clustering at almost the 3σ level. The low level of QSO clustering evolution is more consistent with low $\Omega_\circ$ or high values of biasing ($b_{\mathrm{q}\rho} \simeq b_{\mathrm{g}\rho} \geq 2$).

At intermediate scales ($8-50\ h^{-1}$ Mpc) we have tested the QSO correlation function (at the average redshift of 1.27) against linear CDM predictions normalized to the CMB results of *COBE*. For standard CDM ($\Omega_\circ = 1$, $\Gamma = 0.5$) we find the best fit QSO bias to be $b_{\mathrm{q}\rho}(z=0) = 1.40^{+0.28}_{-0.43}$. Thus there appears to be a narrow range around $b_{\mathrm{q}\rho} \sim 2$, consistent with both the biased evolution and comparisons to *COBE* normalized power spectra, which allows the $\Omega_\circ = 1$, CDM model to survive. An interesting test of the $\Omega_\circ = 1$ model should therefore be possible in a larger data set. We also test ΛCDM, finding a similar bias, $b_{\mathrm{q}\rho}(z=0) = 1.20^{+0.13}_{-0.18}$.

At large scales we find little evidence in the LBQS for the anti-correlation between $40-100\ h^{-1}$ Mpc seen in the Durham/AAT survey. In the combined sample we find no significant signal on any scale larger than $50\ h^{-1}$ Mpc. Since from simulations we estimate that above $100\ h^{-1}$ Mpc our errors are at the ± 0.025 level, these QSO clustering observations represent the most accurate upper limit on the amplitude of large-scale structure from redshift survey data.

Key words: galaxies: clustering – quasars: general – cosmology: observations – large-scale structure of Universe.

1 INTRODUCTION

One of the keys to the use of QSOs as cosmological probes is understanding how they sample the underlying mass distribution. The relationship between QSOs and 'normal' galaxies is a closely associated problem. Considerable effort has been made over the last few years in order to determine how the 'normal' galaxy population traces the mass distribution. It is clear from redshift surveys that different galaxy types have differing clustering statistics, for example, the results from the APM-Stromlo survey show that late and early type galaxies have significantly different correlation-functions (Loveday et al. 1995). Similarly, Park et al. (1994) have found that the amplitude of the power spectrum in the extended CfA galaxy redshift survey is dependent on luminosity. These results imply that at least a large sub-sample of these galaxies cannot trace the mass distribution. The simplest process to explain this phenomena is the peaks-bias formalism of Bardeen et al (1986), which suggests that objects form in the high density peaks of the underlying field. If we consider QSOs in the light of this biasing their low space density and high redshift implies that QSOs sample the highest peaks of the density field (Efstathiou & Rees 1988), the most direct method of testing this assumption is to carry out deep CCD imaging of regions around QSOs in an attempt to observe the associated galaxies.

Many groups have made attempts to investigate the environments of QSOs. Yee & Green (1987) studied a sample of bright radio-loud QSOs and found that at $z \sim 0.6$ QSOs are often found in clusters as rich as Abell richness class 1 clusters. Ellingson, Yee & Green (1991) observed a sample of 63 QSOs with $0.3 < z < 0.6$ where approximately half of the sample was radio-quiet and found a significant difference between the environments of radio-loud and radio-quiet objects. In the radio-quiet sample it was found that the excess population of galaxies around the QSOs did not differ significantly from that expected of a normal galaxy. Hintzen, Romanishin & Valdes (1991) have found an excess of galaxies around radio-loud QSOs at $0.9 < z < 1.5$, while Boyle & Couch (1993) have observed radio-quiet QSOs in the same redshift range and found no excess galaxy population. These results seem to point to a marked segregation between radio-loud and radio-quiet environments with radio-quiet QSOs (which are in the majority) having environments which are similar to that of average galaxies.

The second obvious method to determine how QSOs sample the density field is to look at the clustering statistics of samples of QSOs. The Durham/AAT QSO survey (Boyle 1986) was the first to show small-scale clustering in a well defined sample of QSOs (Shanks el at. 1987). A large scale QSO 'supercluster' was found in the CFHT survey of 215 QSOs (Crampton et al. 1985,1987,1989) at $z = 1.1$ which has dimensions $\simeq 50\ h^{-1}$ Mpc in comoving coordinates. However no significant clustering was found in the remains of the survey. Shanks & Boyle (1994), Paper I, combined the completed Durham/AAT UVX sample (Boyle et al. 1990) with the CFHT survey and the ESO/AAT sample (Boyle, Jones & Shanks 1991; Zitelli et al. 1992) of 83 UVX/colour selected to obtain statistics on a sample of ~ 700 QSOs, finding significant clustering on scales $< 10\ h^{-1}$ Mpc. Boyle & Mo (1993) obtained clustering statistics for the QSOs at low redshift ($z < 0.2$) in the Einstein Extended Medium Sensitivity Survey (EMSS) but did not find a significant clustering signal at small scales. Georgantopoulos & Shanks (1994), Paper II, carried out a similar analysis on the low redshift Seyferts in the IRAS Point Source Catalogue (de Grijp, Miley & Lub 1987) and a 2σ clustering signal was found on scales less than $10\ h^{-1}$ Mpc. Both of these low redshift results are consistent with the amplitude of QSO clustering at $z = 1.4$ if there is no evolution of the clustering in comoving coordinates. These various data point to a low amplitude for QSO clustering at present, and based on the results of Paper I this in turn implies only small amounts of evolution in the clustering of these objects between a redshift of 1.4 and 0.1. If these samples of AGN (both Seyferts and QSOs) do in some reasonably simple way, trace the underlying density field then this lack of evolution has a profound effect on our expectation of how this density field should evolve.

In this paper we present clustering results from the LBQS, together with the Durham/AAT UVX sample, the CFHT objective prism/colour selected sample and the ESO/AAT UVX/colour data (outlined in Croom, Shanks & Boyle 1995). Paper I of this series discusses all of these samples apart from the LBQS and Paper II is concerned with the low z Seyferts from the IRAS PSC. Here we will discuss all four QSO surveys using some new methods of analysis and compare our results to theoretical expectation. We will also compare our conclusions with those of recently published papers looking at some of the same data, namely those of Mo & Fang (1993) and Andreani & Cristiani (1992).

In Section 2 below we briefly discuss the QSO samples themselves, We then go on to discuss the techniques used to calculate the 2-point correlation function for QSOs with particular attention to the errors (Section 3). In Section 4 we present clustering results on small scales (that is $< 10\ h^{-1}$ Mpc), with results on larger scales in Section 5. Section 6 uses a new method based on a simple biased model of evolution to interpret the results from Section 4. In Section 7 we compare CMB normalized CDM power spectrum amplitudes to the QSO clustering. We conclude this paper with a discussion of our results and our conclusions.

2 DATA

2.1 The QSO samples

The LBQS survey (Hewett, Foltz & Chaffee 1995) consists of 18 UKST fields. The magnitude limits in each field vary, $18.41 < B_{J\mathrm{lim}} < 18.85$ mag, a conservative error of 0.15 mag (Foltz et al. 1987) is suggested for the QSO magnitudes. The survey is objective prism selected (plates measured by the APM). The sample contains a total of 1053 QSOs.

The three other QSO surveys considered in this paper are described in Paper I. The largest of these is the Durham/AAT UVX survey (Boyle et al. 1990) with 392 QSOs to a limiting magnitude of $B = 21$ mag in a redshift range $0.3 < z < 2.2$. The ESO/AAT survey (Boyle et al. 1991; Zitelli et al. 1992) is a smaller (83 QSOs within $0.3 < z < 2.2$) and fainter survey, with a limit of $B = 22.5$ mag and was colour/UVX selected. The CFHT survey (Crampton et al. 1989) is objective prism/colour selected and is limited to $B < 20.5$ mag, there are 215 QSOs within the same redshift range as the Durham sample. This last sample has one field (at $12^{\mathrm{h}}48^{\mathrm{m}} + 27^{\circ}$) which may not be statistically representative of the normal QSO distribution on scales $\lesssim 50\ h^{-1}$ Mpc, as this field was chosen to be centred on a previously observed 'QSO supercluster' at $z \simeq 1.1$. When considering this survey we will quote results both with and without the region $0.9 < z < 1.2$ in this field included in our analysis (removing this region rejects 30 QSOs from the sample).

2.2 Comparison of LBQS and other surveys

The LBQS has considerably brighter magnitude limits that the three other surveys. This raises particular problems when considering clustering analysis, the largest problem is the surface density of QSOs. LBQS limited to $B_J \geq 18.41$ mag has an effective area of 453.8 deg^2 (Hewett, Foltz & Chaffee 1993) implying a surface density of 1.47 QSOs deg^{-2}. By comparison the Durham/AAT survey has a surface density of 33.05 QSOs deg^{-2}. The accuracy of $\xi(r)$ is strongly dependent on the number of QSO-QSO pairs at a scale r, it is only when we reach large scales ($\sim 100\ h^{-1}$ Mpc) that the larger number of objects in the LBQS sample is effectively translated into a greater number of pairs than in the Durham/AAT sample, thus at small

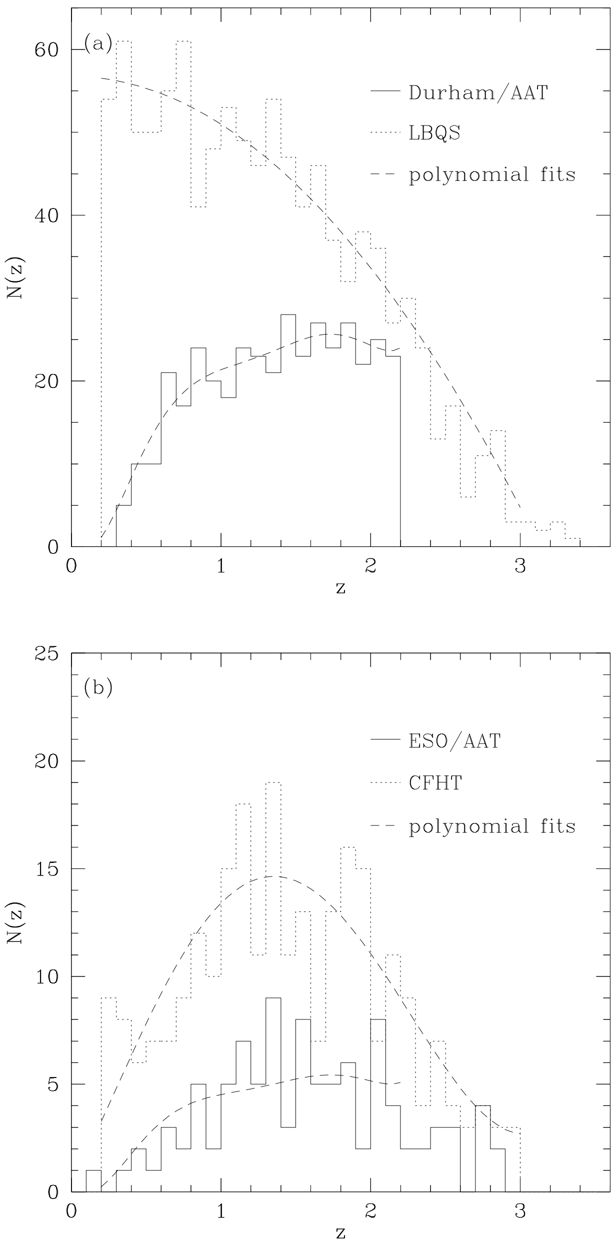

Figure 1. The $N(z)$ distributions for the surveys used in this paper, (a) the Durham/AAT and LBQS samples, and (b) the CFHT and ESO/AAT samples. Each plotted with a fitted polynomial, the first three samples using individual fits and the ESO/AAT using a normalized Durham/AAT fit. These polynomials are used in producing the random samples for our calculations of $\xi(r)$.

scales the Durham/AAT, ESO and CFHT surveys can produce more significant results than the LBQS sample. The bright magnitude limit for LBQS also produces a very different form of N(z) to that of the fainter surveys with many more objects at lower redshifts (see Fig. 1). Although the LBQS extends to $z > 3$, in order to be consistent with the other surveys we will generally consider the LBQS to a limiting redshift of $z = 2.2$.

3 TECHNIQUES

3.1 Correlation Function Estimates

On the scales that we can probe with the QSO 2-point correlation function (ξ) separation is strongly dependent on cosmology. We use the method of Osmer (1981) which uses the coordinate transformation in the Robertson-Walker metric,

$$\mathbf{X}' = \mathbf{X} + \mathbf{a}[\sqrt{1 - k\mathbf{X}^2} - (1 - \sqrt{1 - k\mathbf{a}^2})(\mathbf{X}.\mathbf{a}/\mathbf{a}^2)] \qquad (1)$$

Where $\mathbf{a} = (0, 0, s_1)$ and $\mathbf{X} = (s_2 \sin(\theta), 0, s_2 \cos(\theta))$, with s_1 and s_2 the dimensionless comoving distance to QSO 1 and 2 respectively, and θ is their angular separation on the sky. This is a relatively simple transformation, however the values s_1 and s_2 depend on the cosmological model used. For a general cosmology (including a cosmological constant) we find s for a redshift z via,

$$x = \frac{1}{a_\circ} \int_0^z \frac{\mathrm{d}z}{\sqrt{A(1+z)^3 + B(1+z)^2 + C}} \qquad (2)$$

(Refsdal 1966) with

$$A = \Omega_\circ, \;\; B = -(\frac{3}{2}\Omega_\circ - q_\circ - 1), \;\; C = \frac{\Omega_\circ}{2} - q_\circ \qquad (3)$$

then

$$s = \begin{cases} \sin(x) & k = 1 \\ x & k = 0 \\ \sinh(x) & k = -1 \end{cases} \qquad (4)$$

When we are considering $\Lambda = 0$ then we can solve exactly, obtaining

$$s = \frac{zq_\circ + (q_\circ - 1)(\sqrt{2zq_\circ + 1} - 1)}{(1+z)q_\circ^2} \qquad (5)$$

For $\Lambda \neq 0$ the integral can only be solved numerically, however in Paper I an approximation was used (Peebles 1984) for inflationary Λ models,

$$s = z \text{ for } 1 + z < (\Omega_\circ^{-1} - 1)^{1/3} \qquad (6)$$

The correlation function is a difference of two comoving distances, so an assumed cosmology will effect ξ via $\mathrm{d}s/\mathrm{d}z$. In Fig. 2 we plot the relative $\mathrm{d}s/\mathrm{d}z$ compared to an $q_\circ = 0.5$ universe for some different cosmologies. The above approximation for inflationary Λ is only exact for $\Omega_\circ = 0$, for $\Omega_\circ = 0.03$ the approximation deviates from the true value by 10 per cent at $z = 1$ and 34 per cent at $z = 2$. Once $\mathbf{X}'$ is found (equation (1)), the comoving separation is,

$$r = \frac{c}{H_\circ} \begin{cases} \operatorname{arcsin}(|\mathbf{X}'|) & k = 1 \\ |\mathbf{X}'| & k = 0 \\ \operatorname{arcsinh}(|\mathbf{X}'|) & k = -1 \end{cases} \qquad (7)$$

The estimator used to produce the 2-point correlation function is

$$\xi(r) = \frac{N_{\mathrm{qq}}}{N_{\mathrm{qr}}} \frac{2n_{\mathrm{r}}}{(n_{\mathrm{q}} - 1)} - 1 \qquad (8)$$

where N_{qq} is the number of QSO pairs of separation $r - \delta r/2$ to $r + \delta r/2$ and N_{qr} is the number of QSO random pairs in the same interval. The second term has the effect of normalizing $\xi(r)$, n_{q} is the number of QSOs and n_{r} the number of random points, we generally use $n_{\mathrm{r}} = 100n_{\mathrm{q}}$ within each field. As the magnitude limits for each LBQS field differ the number of random points is normalized to the number

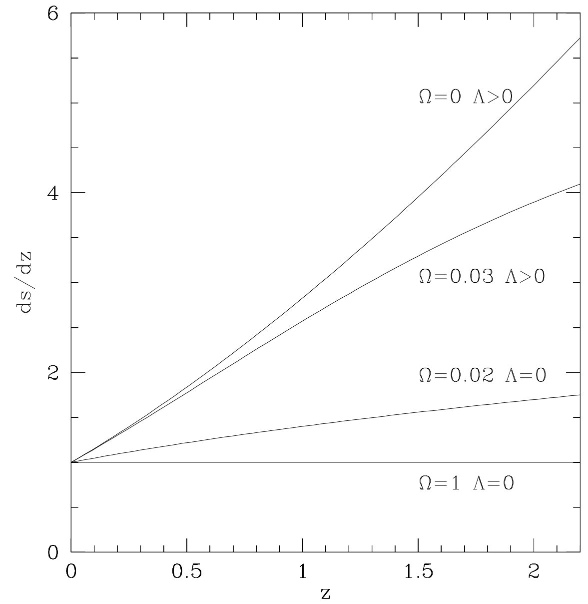

Figure 2. $\mathrm{d}s/\mathrm{d}z$ as a function of redshift, normalized to $\mathrm{d}s/\mathrm{d}z$ for a $q_0 = 0.5$, where s is the comoving distance. This is plotted for some of the cosmologies used in this paper, namely $q_0 = 0.5$ and $q_0 = 0.01$ with $\Lambda = 0$ and flat low Ω_0 models with $\Lambda \neq 0$.

of QSOs in the individual fields. We give each point a random RA, declination and a random redshift weighted by the overall $N(z)$ for the QSO sample.

A comment is required concerning the variable effective area in different LBQS fields. All the LBQS fields cover $5.8° \times 5.8°$, however, each field has different regions removed due to overlapping spectra, stepwedges and bright objects (Hewett et al. 1995). We calculate $\xi(r)$ for the LBQS by two different methods, the first is to simply take the $5.8° \times 5.8°$ area (apart from those fields which overlap, where the overlaps are removed from one of the fields) and distribute randoms within this region with no regard to any holes in the effective area. The second is to use the real positions of the LBQS QSOs for our random points, but randomly shuffle their redshifts, we then use 1000 realisations of this process to obtain a mean number of QSO-random pairs. When we compare the two processes we find no significant difference, the rms difference between the two estimates is 0.26σ where σ is the error on the first estimator. Throughout this paper we will use the first of the estimators.

No correlation between Schmidt fields is attempted, as any systematic magnitude calibration error between fields would mean a considerable QSO density variation. If we use a form for the bright counts such that $N(<B) \propto 10^{0.8B}$ then a ~ 0.1 mag error in the zero point magnitude produces a 20 per cent variation in the QSO surface density. Our normalization is such that it forces the integral correlation function to zero on the very largest scales probed. On small scales we also use $\bar{\xi}(r)$ where,

$$\bar{\xi}(r) = \frac{3}{r^3}\int_0^r \xi(x)x^2\mathrm{d}x \qquad (9)$$

To estimate this we simply use the same estimator as for ξ, but for pairs at separation 0 to r.

3.2 Error Analysis

3.2.1 *Field-to-field variation*

We look at the field-to-field variance of the number of QSOs in the LBQS. We take the 18 fields and consider the number counts of QSOs to a limiting magnitude of $B_{\mathrm{Jlim}} = 18.41$ mag. We carry out a χ^2 test on the hypothesis that the fields are derived from the same population. The result is $\chi^2 = 33.92$ for 17 degrees of freedom, this is a rejection of the hypothesis at a 99 per cent significance level. Most of this variation comes from three fields, two equatorial, $01^{\mathrm{h}}00^{\mathrm{m}} - 00°00'$, $22^{\mathrm{h}}40^{\mathrm{m}} - 00°00'$ and one southern $00^{\mathrm{h}}53^{\mathrm{m}} - 28°00'$ with 56, 24 and 57 QSOs respectively. Without these fields a χ^2 test gives $\chi^2 = 16.47$ on 14 degrees of freedom, only significant at the 70 per cent level. A possible cause of this effect could be residual magnitude errors after calibration, although CCD sequences were used to obtain zero-points and linearize the APM magnitudes, there could still be systematic variations across individual fields of up to 0.1 mag (Hewett et al. 1995). We feel that this justifies our choice to not correlate QSOs between individual fields.

3.2.2 *Correlation function errors*

Analysis of errors in the two-point correlation function is an area of intense debate. At small scales we have a small number of pairs, while at the largest scales we can probe $\xi(r)$ has an intrinsically lower amplitude causing any signal to be close to the noise. To determine our errors, particularly on larger scales, we have carried out an analysis of several different error estimators to find the most accurate and consistent errors for our estimates of the QSO $\xi(r)$. We consider Poisson, field-to-field, simulated and bootstrap (Barrow, Bhavsar & Sonoda 1984) methods to produce estimates for the error on the QSO correlation function.

The Poisson noise due to the number the pairs in the sample is

$$\Delta\xi = \frac{1+\xi}{\sqrt{N_{\mathrm{qq}}}} \qquad (10)$$

at smaller scales where the number of pairs is small and most pairs are independent. At large scales, where pairs of QSOs are not independent n_{q} should be more realistic than N_{qq}.

For field-to-field errors we split the LBQS survey up into five regions, each containing ~ 170 QSOs. We produced multiple random simulations (a good approximation to the survey due to the small number of correlated pairs) of the LBQS survey region. We also take bootstrap resamplings and find a variance from this process. For each of the simulation and bootstrap methods we take 100 realisations.

In Fig. 3 we plot our error estimates normalized to the Poisson ($\sqrt{N_{\mathrm{qq}}}$) error for the LBQS sample. The field to field variance has a large scatter over all scales probed by the LBQS $\xi(r)$, but $\Delta\xi_{\mathrm{field-field}}/\sqrt{N_{\mathrm{qq}}}$ is consistent with $\simeq 1$ at all these scales. The variance calculated from simulations is also consistent with Poisson errors on all scales. The error resulting from the bootstrap method produces errors that are 1.7 times larger than the $\sqrt{N_{\mathrm{qq}}}$ at all scales. This is consistent with a suggested analytical expression for the bootstrap error (Mo, Jing & Borner 1992),

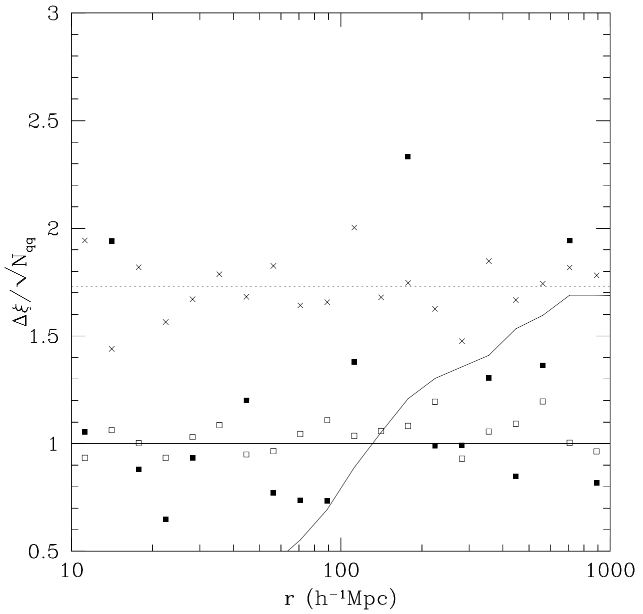

Figure 3. Relative estimates of the errors in the 2-point correlation function from simulations (open squares), field-to-field variation (filled squares), bootstrap resampling (crosses), and $n_{\rm q}$ (solid line), normalized to $N_{\rm qq}$ for the LBQS sample. The dotted line is $(\Delta\xi)^2 = 3N_{\rm qq}$.

$$\sigma^2_{\rm boot}(r) \simeq 3N_{\rm qq}(r) + \frac{4N^2_{\rm qq}(r)}{n_{\rm q}} \tag{11}$$

This expression was formulated assuming a large contiguous region in which the edge effects are negligible, this is obviously not the case for any of the QSO surveys. As a result we find that the second term in the above expression is always small, particularly as we do not cross correlate between fields. Hence we find $\Delta\xi_{\rm boot}/\sqrt{N_{\rm qq}} \simeq \sqrt{3}$ at all scales.

At small scales we know that the bootstrap errors over estimate the true errors we should therefore use $\sqrt{N_{\rm qq}}$ errors on these scales as they are consistent both field-field and simulation errors. On larger scales ($> 100\ h^{-1}$ Mpc) the choice is not so obvious, bootstrap errors should be more realistic on these scales but these still over estimate the field-field and simulated errors by a factor of $\sqrt{3}$. $n_{\rm q}$ errors are consistent with $N_{\rm qq}$ errors at $\sim 100\ h^{-1}$ Mpc and consistent with bootstrap estimators at $\sim 1000\ h^{-1}$ Mpc. For these reasons (and because of the large amount of time needed to run simulations for every case) we will plot $\sqrt{N_{\rm qq}}$ errors until $N_{\rm qq} = n_{\rm q}$ then use $\sqrt{n_{\rm q}}$. It should be noted that the majority of our analysis will be carried out below 50 h^{-1} Mpc and in this region it is clear that $\sqrt{N_{\rm qq}}$ is the best choice. When looking for low amplitude signals at larger scales we will use the simulations to obtain a reliable estimate of the uncertainty.

4 RESULTS AT SMALL SCALES

We show a comparison of the four surveys in Fig. 4. Figs. 4(a) and 4(b) show the correlation functions for LBQS and Durham/AAT on log-log plots for $q_\circ = 0.5$. The LBQS in particular does not have a strong signal at small scales.

Table 1. The integrated QSO clustering, $\bar{\xi}$, within 10 h^{-1} Mpc and 25 h^{-1} Mpc, for the LBQS and for all surveys combined (excluding the CFHT 'cluster'), for various cosmologies.

$\Omega_\circ$	$\lambda_\circ$	LBQS $\bar{\xi}(10)$	All $\bar{\xi}(10)$	All $\bar{\xi}(25)$
1	0	1.86 ± 1.28	0.83 ± 0.29	0.16 ± 0.08
0.1	0	1.06 ± 1.45	1.09 ± 0.47	0.21 ± 0.11
0.02	0	1.09 ± 1.48	1.01 ± 0.50	0.28 ± 0.12
0.2	0.8	2.42 ± 2.42	1.01 ± 0.58	0.35 ± 0.14
0.03	0.97	1.54 ± 2.55	0.76 ± 0.79	0.74 ± 0.23

We see that the two surveys both appear to be consistent with the power law plotted, that is $\xi(r) = (r/6)^{-1.8}$. In Fig. 4(c) we plot the the combined QSO $\xi(r)$ for the ESO/AAT and CFHT samples which has been plotted in paper I. However, it should be noted that *re-analysis* of this data has shown an inaccuracy in the $\xi(r)$ of these two surveys reported in Paper I. We find that the signal at small scales was over-estimated and the anti-correlation reported at $40 - 100\ h^{-1}$ Mpc (see Section 5) is found to be less significant. Fig. 4(c) shows a corrected version of the combined CFHT and ESO/AAT $\xi(r)$ and this plot now shows some excess power on $20 - 40\ h^{-1}$ Mpc scales compared to the $r_\circ = 6\ h^{-1}$ Mpc power law, as we might expect from the CFHT 'supercluster'. When this region is removed (the open symbols in Fig. 4(c)) the excess power is reduced, particularly at 30 h^{-1} Mpc. Taking all four surveys and combining them using pair weighting we obtain Fig. 4(d) where the correlation function is consistent with $\xi(r) = (r/6)^{-1.8}$.

In Paper I it was found that $\bar{\xi}(10\ h^{-1}\ {\rm Mpc}) = 0.93 \pm 0.34$ for Durham/AAT, CFHT (without cluster) and ESO/AAT combined. With the corrected analysis for CFHT and ESO/AAT this becomes $\bar{\xi}(10) = 0.74 \pm 0.30$. For the LBQS individually we find $\bar{\xi}(10) = 1.86 \pm 1.28$ (there are only 5 QSO-QSO pairs within 10 h^{-1} Mpc) and combining this with the other surveys we have $\bar{\xi}(10) = 0.83 \pm 0.29$. We show these results in Table 1 along with results for different cosmologies. This is the best current estimate of the QSO clustering amplitude at high z. The mean redshift of the combined sample is $z = 1.27$.

Formally the significance of a rejection of a Poisson random distribution is 3.8σ (by comparing 39 pairs found to 21.3 expected). In cosmologies with low $\Omega_\circ$, we generally find a higher amplitude but larger errors, as pairs move out to larger scales. For $q_\circ = 0.01$ $\bar{\xi}(10) = 1.01 \pm 0.50$ (considering the whole sample without the CFHT cluster) and for $\Omega_\circ = 0.2$ and $\lambda_\circ = 0.8$ (where $\lambda = \Lambda c^2/3H_\circ^2$) we find $\bar{\xi}(10) = 1.01 \pm 0.58$, representing a formal detection of clustering at the 2.8σ and 2.5σ levels respectively. If we split the combined sample ($q_\circ = 0.5$) into redshift bins we find that for $0.3 < z < 1.4$, $\bar{\xi}(10) = 0.97 \pm 0.43$ and for $1.4 < z < 2.2$ $\bar{\xi}(10) = 0.68 \pm 0.40$. Although the high redshift signal is lower there is no significant evolution between the two redshift bins.

5 RESULTS AT LARGE SCALES

Now we look at the large scale clustering of the LBQS and other samples assuming various cosmologies, in particular

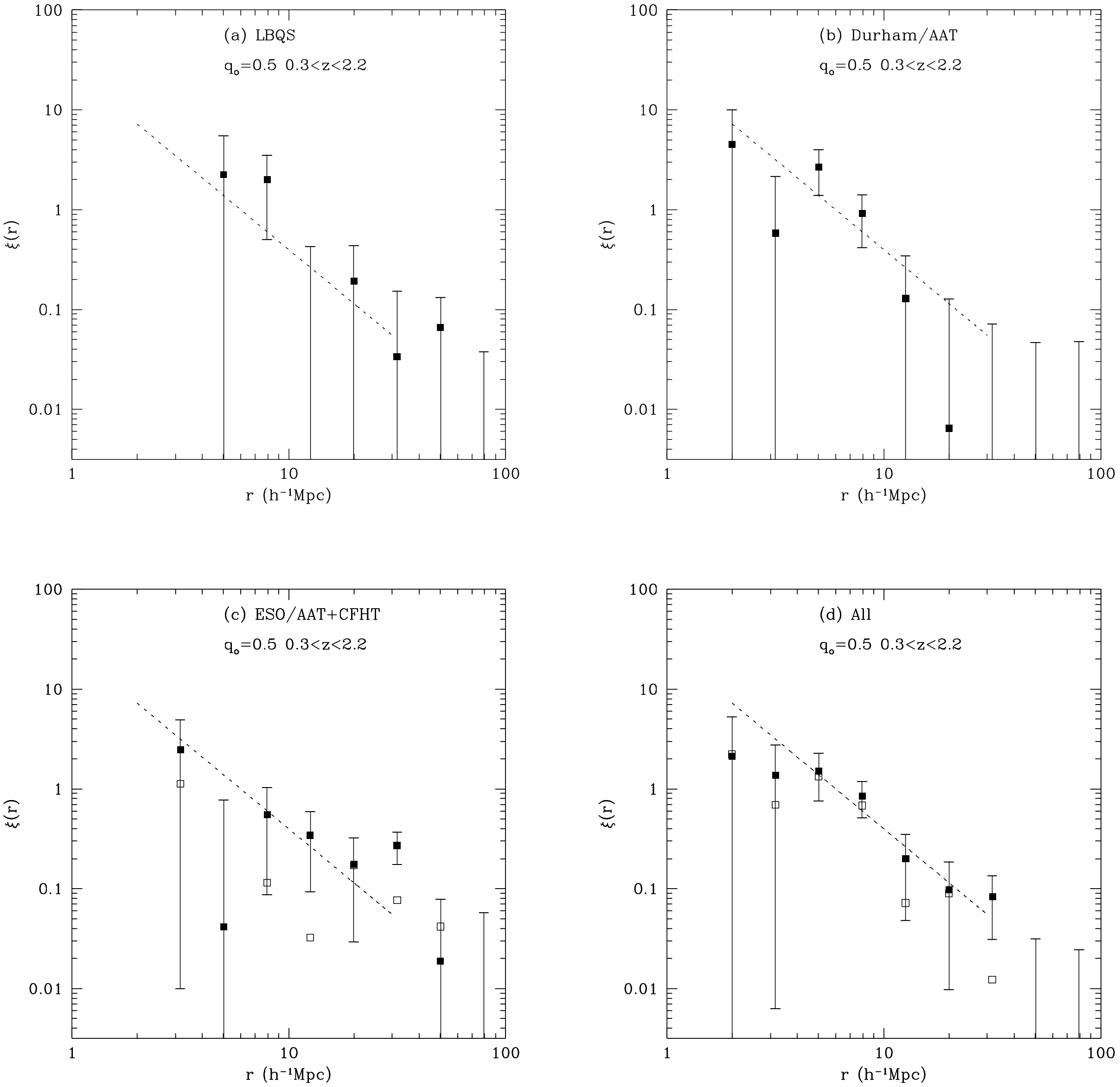

Figure 4. QSO correlation functions on small scales for a $q_\circ = 0.5$ flat cosmology in the redshift range $0.3 < z < 2.2$, (a) the LBQS, (b) the Durham/AAT sample, (c) the corrected ESO/AAT and CFHT combined (open squares with the redshift range $0.9 - 1.2$ removed in the $12^{\rm h}48^{\rm m} + 27^\circ$ field) and (d) all surveys combined (again the open symbols are with the CFHT 'supercluster' removed).

two with zero Λ ($q_\circ = 0.5$ and $q_\circ = 0.01$) and one flat model with $\Lambda \neq 0$ and $\Omega_\circ = 0.03$ which is consistent with baryon nucleosynthesis. Combining the LBQS survey with the Durham/AAT, ESO/AAT and CFHT surveys from paper I to get a sample of > 1500 QSOs. We have small errors out to scales of $\sim 1000\ h^{-1}$ Mpc, however any signal at these scales will also be small.

5.1 Contribution of LBQS at larger scales

In Section 4 we pointed out that the LBQS makes very little contribution on scales less than $\sim 10\ h^{-1}$ Mpc. However on larger scales the LBQS is a strong probe of structure, the counts of QSO pairs peaks at over $600\ h^{-1}$ Mpc and extends well past $1000\ h^{-1}$ Mpc.

We wish to compare and combine the LBQS $\xi(r)$ with the Durham/AAT sample and others, so we have calculated the LBQS $\xi(r)$ in the same redshift region as for these samples, namely $0.3 < z < 2.2$ (Fig. 5(a)). We see no significant large scale features at any scale, but

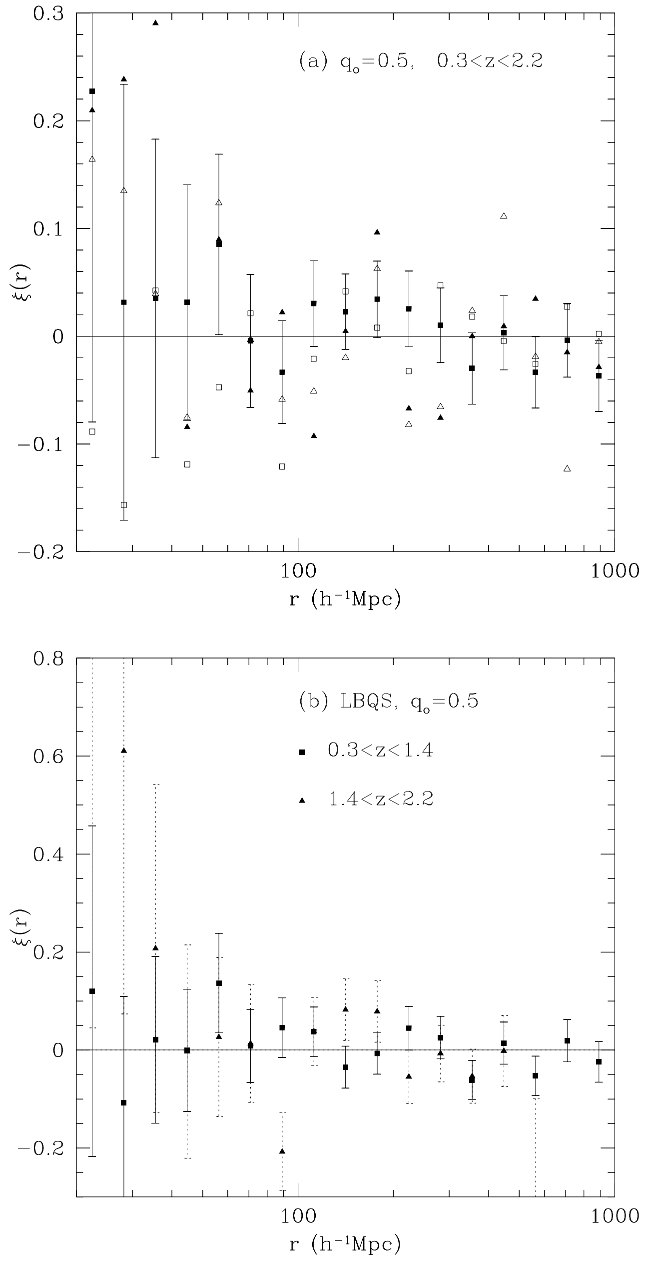

Figure 5. QSO Correlation functions with $q_o = 0.5$ and $0.3 < z < 2.2$, (a) the LBQS (filled squares with errors), Durham/AAT (open squares) and re-analysed CFHT and ESO/AAT (filled triangles, open triangles with CFHT 'supercluster' removed). (b) $\xi(r)$ for LBQS in redshift bins $0.3 < z < 1.4$ (filled squares) and $1.4 < z < 2.2$ (filled triangles)

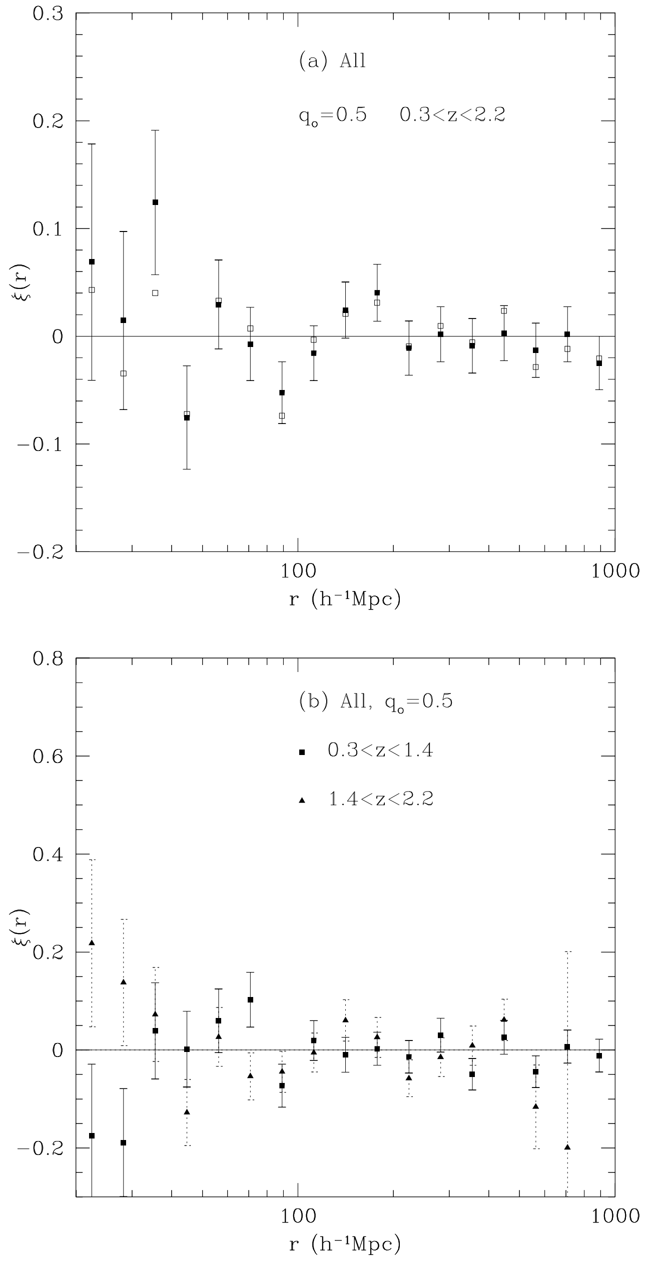

Figure 6. The QSO correlation function for the entire combined sample, for $q_o = 0.5$. (a) Redshift range $0.3 < z < 2.2$ (open squares with the CFHT 'supercluster' removed), (b) $0.3 < z < 1.4$ without CFHT 'supercluster' (filled squares) and $1.4 < z < 2.2$ (filled triangles).

we should like to ask if this is consistent with the other surveys at these scales. An anti-correlation is seen in the $40 - 100\ h^{-1}$ Mpc region of the Durham/AAT sample at the 2σ level (Paper I and open squares in Fig. 5(a)). It is clear that there is no anti-correlation at this scale in the LBQS. The value found in Paper I for the Durham/AAT sample was $\xi(40 - 100\ h^{-1}\ \mathrm{Mpc}) = -0.084 \pm 0.036$ (simulation errors), whereas in the LBQS $\xi(40 - 100\ h^{-1}\ \mathrm{Mpc}) = 0.00 \pm 0.034$ (simulation errors), this is only a significant difference at $< 2\sigma$. We also plot the revised estimate for $\xi(r)$ in the CFHT and ESO/AAT samples, in this case the signal in the $40 - 100\ h^{-1}$ Mpc region is -0.006 ± 0.041. Comparing the point in the Durham/AAT survey at 89 h^{-1} Mpc to the LBQS we find that at this scale the LBQS ξ is not significantly negative (-0.033 ± 0.048). We find no evidence in the clustering of the LBQS to support the claimed anti-correlation of Paper I, although the two results do not strongly disagree.

We next split the LBQS survey into redshift bins, for consistency using the same bins as Paper I, that is $0.3 < z < 1.4$ and $1.4 < z < 2.2$ and produced correlation functions for

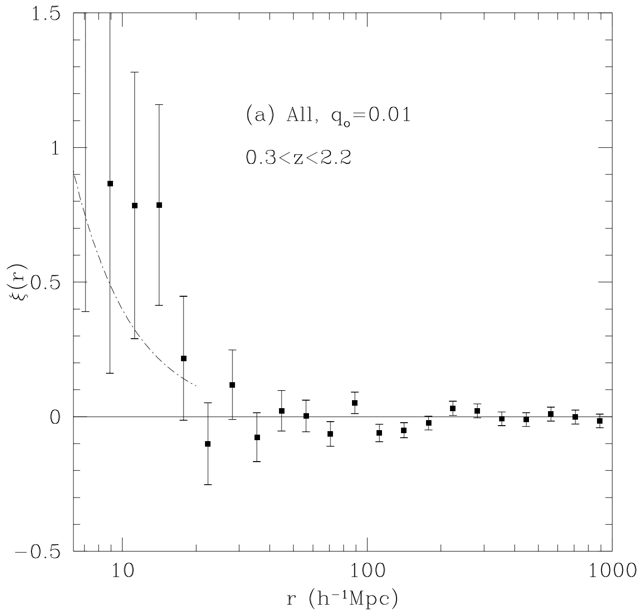

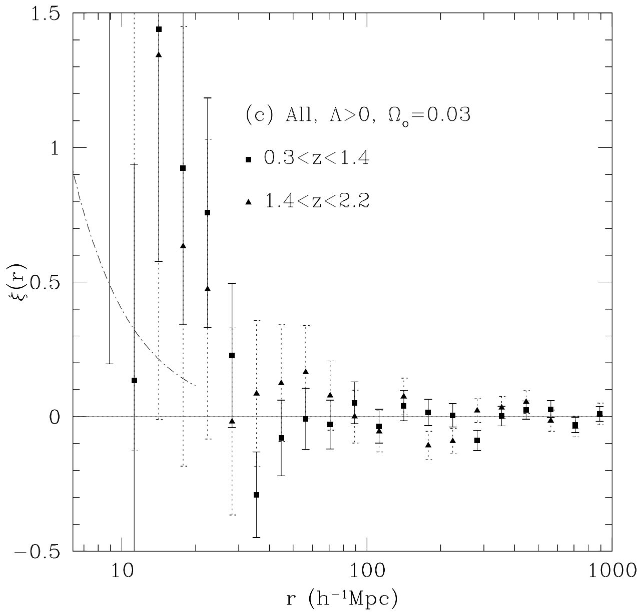

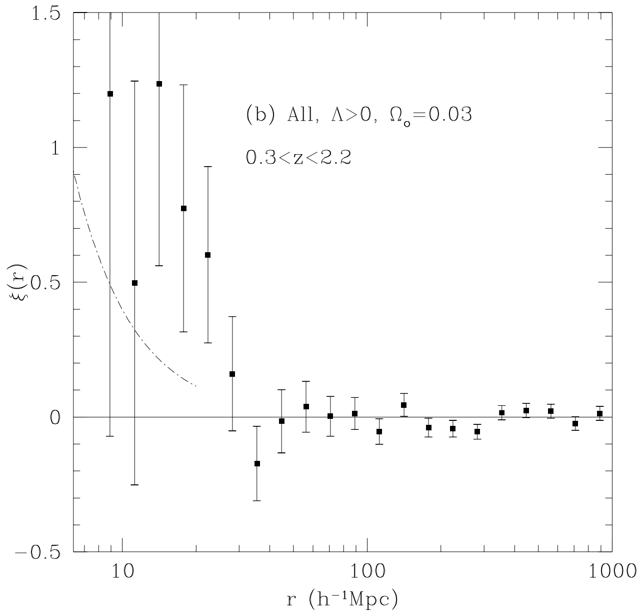

Figure 7. The QSO correlation function for the entire combined sample with (a) $q_{\circ} = 0.01$, (b) inflationary Λ, $\Omega_{\circ} = 0.03$, $\lambda_{\circ} = 0.97$ and (c) inflationary Λ, $0.3 < z < 1.4$ (filled squares) and $1.4 < z < 2.2$ (filled triangles). For clarity we only plot points excluding the CFHT 'supercluster'. In all cases the dot-dashed line is $\xi = (r/6)^{-1.8}$.

these (see Fig. 5(b)). In the $0.3 < z < 1.4$ case there are 556 QSOs, again we see very little structure, there are no significant deviations from zero at any scale. In the Durham/AAT sample the anti-correlation was largely at low redshifts, but no sign of it is seen here. By contrast we do see a signal at 89 h^{-1} Mpc in the high redshift data, $\xi(r) = -0.21 \pm 0.08$.

5.2 Large-scale structure in a combined sample of QSOs

It is not until $\sim$ 100 h^{-1} Mpc that the LBQS becomes more statistically powerful than the Durham/AAT survey, since up to this point the Durham/AAT sample has more pairs per bin than the LBQS. We combine these two surveys together with the ESO/AAT sample and the CFHT survey, using a simple pair weighting. The combined $\xi(r)$ is shown in Fig. 6(a), constituting one of the most accurate available representations of large-scale structure on scales in excess of 50 h^{-1} Mpc. Removing the CFHT 'supercluster' does make some considerable difference out to scales $\sim$ 30 h^{-1} Mpc, but at any scale greater this there is little effect. In the region at $40 - 100$ h^{-1} Mpc that caused interest in the Durham/AAT sample the mean correlation function is now $\xi(40 - 100\ h^{-1}\ \mathrm{Mpc}) = -0.026 \pm 0.022$ (this error is obtained from simulations, note that $\sqrt{n_{\rm q}}$ would give a similar error, ± 0.024). When we look more closely at the region around 100 h^{-1} Mpc there are points at 89 and 177 h^{-1} Mpc that are marginally ($1.5 - 2\sigma$) from zero so this can only be taken as tentative evidence of a feature. Positive signals near these scales have been seen in pencil-beam galaxy surveys (Broadhurst et al. 1990) which have very similar geometry to all the QSO surveys we use, so there is some observational precedent for a signal of this kind. On scales greater than 200 h^{-1} Mpc we see no deviation away from a Poisson distribution. Splitting the combined sample into redshift bins, Fig. 6(b), we see that both redshift bins contribute to the signal at $\sim$ 100 h^{-1} Mpc but no distinctive features are seen.

5.3 QSO $\xi(r)$ in low $q_{\circ}$ and $\Lambda \neq 0$ models

In Fig. 7 we present the combined QSO correlation function assuming $q_{\circ} = 0.01$ (Fig. 7(a)) and for a flat universe with a positive cosmological constant and $\Omega_{\circ} = 0.03$ (Fig. 7(b)). Fig. 2 shows how the differential comoving distance varies with cosmology, this effect can be used to discriminate between cosmologies if we can observe linear features in the correlation function at low redshift. Linear theory predicts that features should not change scale as they evolve, their only evolution is in amplitude. Hence if we observe a low redshift feature in the correlation function then search for it in a higher redshift sample, we should find it at the same scale in both regimes. Effectively we are using features in the correlation function as standard rods (see Paper I). Both low $q_\circ$ and positive Λ increase the average separation between pairs of QSOs. To quantify this we calculate $\bar{\xi}(25\ h^{-1}$ Mpc) for these three cases (see Table 1), for $q_\circ = 0.5$ $\bar{\xi}(25) = 0.16 \pm 0.08$, for $q_\circ = 0.01$, $\bar{\xi}(25) = 0.28 \pm 0.12$, and for inflationary Λ, $\bar{\xi}(25) = 0.74 \pm 0.23$ (all these without the CFHT 'supercluster'). In Fig. 7(c) we plot the QSO $\xi(r)$ with inflationary Λ for our two redshift bins in an attempt to pick out features. From low to high redshift we expect a doubling of the scale of any real feature, if $q_\circ = 0.5$ is the correct cosmology. At some level this will be watered down by the angular separation of the QSOs, but all the samples considered in this paper are of a geometry which is much more extended in the radial direction. We see an anti-correlation $\xi = -0.088 \pm 0.037$ in the 280 h^{-1} Mpc bin at low redshift. At high redshift we see a feature at $\sim 200\ h^{-1}$ Mpc, the combined signal from the two bins either side of 200 h^{-1} Mpc is -0.098 ± 0.035. We generally expect a signal to move to larger scales with increasing redshift, this is not the case for these two points, this therefore suggests that the two negative points are not caused by the same feature.

At smaller scales $\bar{\xi}(25) = 0.74 \pm 0.23$ (0.95 ± 0.24 with the CFHT cluster) at $z = 1.27$ in the Λ model can be compared to a power law with $r_\circ = 6\ h^{-1}$ Mpc and slope of -1.8 (making the simplifying assumption that this power law extends to $\sim 25\ h^{-1}$ Mpc). We find them to be inconsistent at the 2.9σ (4σ with CFHT 'supercluster'). If QSOs randomly sample the galaxy distribution (see arguments below), this is then a rejection of the Λ model. We assume ξ is approximately stable in comoving coordinates as a function of z, if ξ did in fact evolve faster the rejection would be stronger. Similarly if the power law turned over before 25 h^{-1} Mpc then the present day clustering amplitude would be lower, again increasing the significance of the rejection. We attempted the same analysis for a low $q_\circ$ cosmology ($q_\circ = 0.01$) but we did not find a significant rejection.

6 A SIMPLE MODEL FOR BIASED CLUSTERING EVOLUTION

At scales of $\sim 10 - 20\ h^{-1}$ Mpc the amplitude of the QSO correlation function is such that we may start to discriminate between evolutionary models of large-scale structure. In particular, the redshift evolution of the mass correlation function depends strongly on $\Omega_\circ$. If QSOs are biased with respect to the overall mass distribution, this biasing will play a major role in the evolution of QSO clustering. Mo & Fang (1993) have used both the Durham/AAT and CFHT samples to find an equivalent present day correlation length for QSOs of $r_\circ(z=0) = (18 \pm 2)\ h^{-1}$ Mpc by assuming unbiased linear theory, that is $\delta\rho/\rho \propto (1+z)^{-1}$ (for $\Omega_\circ = 1$) which implies $\xi(z) = \xi(0)/(1+z)^2$. This leaves us with a paradox: this high present day amplitude suggests that the QSOs are highly biased with respect to the present day galaxies and hence to the mass distribution, yet the result is obtained by assuming that the QSO correlation function will evolve in the same manner as the mass correlation function. Similarly,

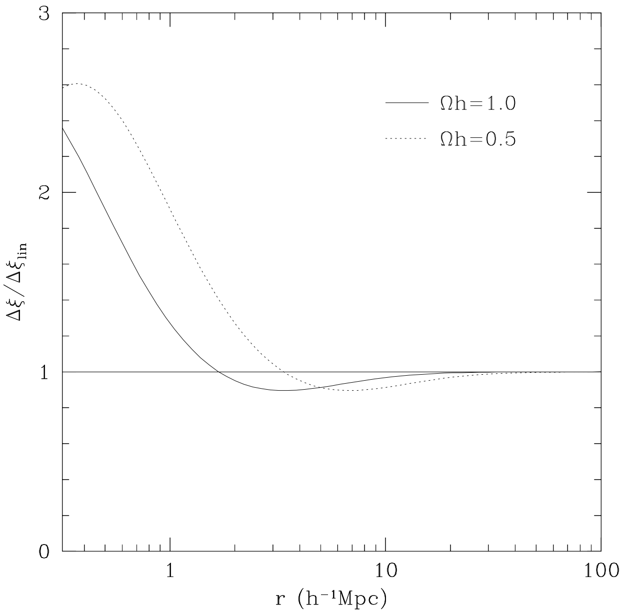

Figure 8. Growth of CDM $\bar{\xi}(r)$ for $\Omega_\circ = 1$ and $h = 0.5, 1$ in the quasi-linear regime, from $z = 1.27$ to the present. Normalized to linear theory evolution, $(1+z)^2$.

evolution which is stable in comoving coordinates (Paper I) is only consistent with linear theory for high biasing or when $\Omega_\circ < 1$. Below we will construct a simple and consistent model of QSO clustering evolution, we can then compare directly to the low z Seyfert result and reject cases for which the two results are inconsistent. We will consider clustering in the linear regime, and use the peaks-bias formalism. We do not use this formalism in the sense that QSOs are rare, therefore very high peaks, and therefore strongly clustered. We are simply stating that above a given threshold QSOs are able to form, but may only form in a *random fraction* of the peaks that are above that threshold. Bardeen et al (1986) defines the bias parameter b as,

$$b = \frac{\langle\bar{\nu}\rangle}{\sigma(t)} + 1 \tag{12}$$

where $\sigma(t)$ is the rms fluctuation in the mass distribution and $\langle\bar{\nu}\rangle$ defines some threshold above which QSOs/galaxies can form. If we assume that $\langle\bar{\nu}\rangle$ is a constant then the dependence of b on redshift is contained in $\sigma(t)$, this will scale as $\delta\rho/\rho$ and hence $b = B(1+z)+1$ where B is some constant, for an $\Omega_\circ = 1$ universe. We now have a form for the evolution but we only have one point, at $z = 1.27$ (if we split the data into redshift bins we obtain no gain because of the increased errors), and we need a comparison at a different redshift to constrain our model. We use the present day ($z = 0$) galaxy correlation function ($\xi_{\rm gg} = (r/6)^{-1.8}$, $\bar{\xi}(10) = 1.00$) as an estimate of the present day mass ξ, at the very least this should be an upper limit to $\xi_{\rho\rho}$. Using linear theory we find,

$$\xi_{\rm qq}(r,z) = [B(1+z)+1]^2 \xi_{\rho\rho}(r,z) \tag{13}$$

and

$$\xi_{\rho\rho}(r,0) = (1+z)^2 \xi_{\rho\rho}(r,z) \tag{14}$$

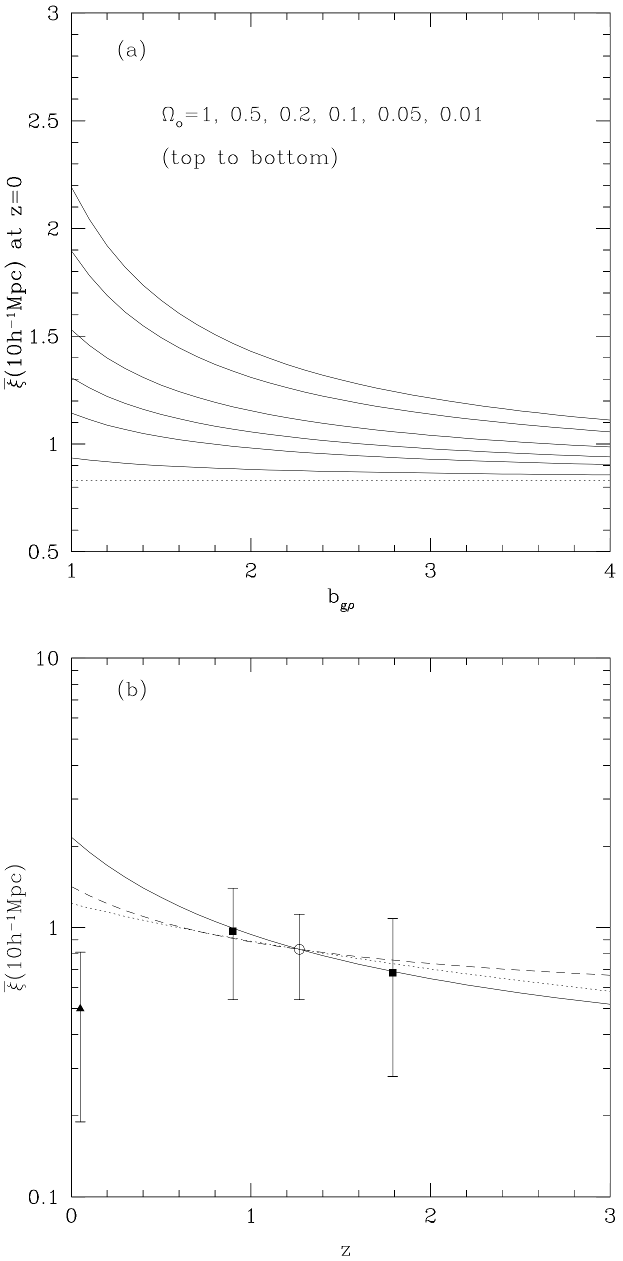

Figure 9. Amplitude of $\bar{\xi}(10\ h^{-1}$ Mpc) assuming our simple biasing model for (a) the combined QSO sample evolved to $z=0$ as a function of $\Omega_\circ$ and $b_{g\rho}$, and (b) the expected evolution in our biasing model for $\Omega_\circ=1$, $b_{g\rho}=1$ (solid line), $\Omega_\circ=1$, $b_{g\rho}=2$ (dashed line) and $\Omega_\circ=0.1$, $b_{g\rho}=1$ (dotted line). The points are the combined QSO clustering result $0.3<z<2.2$ (open circle), combined QSO clustering in two redshift bins $0.3<z<1.4$ and $1.4<z<2.2$ (filled squares) and the low redshift AGN clustering amplitude (Georgantopoulos & Shanks 1994; Boyle & Mo 1993) (filled triangle).

we can also take into account the biasing of the observed galaxy distribution with respect to the mass using

$$\xi_{\rho\rho}=\xi_{gg}/b_{g\rho}^2 \qquad (15)$$

Table 2. Estimates of $b_{q\rho}$, $\bar{\xi}_{qq}(10)$ and $r_\circ$ at $z=0$. Predicted using our biasing model and $\bar{\xi}(10)$ at $z=1.27$.

$\Omega_\circ$	$b_{g\rho}$	$b_{q\rho}(z=0)$	$\bar{\xi}_{qq}(10,z=0)$	$r_\circ(z=0)$
1	1	1.47 ± 0.16	2.16 ± 0.47	9.23 ± 1.11
1	2	2.38 ± 0.32	1.42 ± 0.38	7.30 ± 1.08
0.1	1	1.27 ± 0.23	1.62 ± 0.57	7.85 ± 1.54
0.1	2	2.31 ± 0.45	1.34 ± 0.52	7.08 ± 1.53
0.02	1	1.09 ± 0.25	1.19 ± 0.54	6.62 ± 1.68
0.2(Λ)	1	1.42 ± 0.29	2.00 ± 0.82	8.84 ± 2.00

where $b_{g\rho}$ is the biasing of the galaxies with respect to the mass at $z=0$. Combining these equations we obtain an estimate for $b_{q\rho}$, the estimated present day biasing for QSOs,

$$b_{q\rho}=B+1=\left[\frac{\xi_{qq}(z)}{\xi_{gg}(0)}\right]^{1/2}b_{g\rho}-\frac{1}{1+z}+1 \qquad (16)$$

In our analysis we will use $\bar{\xi}(10\ h^{-1}$ Mpc) rather than ξ as at small scales the QSO $\xi(r)$ is very noisy. Hamilton et al (1991) finds an empirical fit to the non-linear growth of the CDM correlation function. We use this to predict the deviation away from linear theory expected over the range of scales that we are interested in. Fig. 8 shows the relative growth of $\bar{\xi}$ from $z=1.27$ to $z=0$ for two CDM models ($\Omega_\circ=1$ and $h=1,0.5$). We find that the non-linear effects are at the 3 per cent level at 10 h^{-1} Mpc for $h=1$ and at the 9 per cent level for $h=0.5$. Here we are using a CDM correlation function that is normalized to fit a -1.8 power law at $z=0$.

So at $\sim 10\ h^{-1}$ Mpc the linear approximation is close to the expected mass evolution and in particular the error which might be caused by non-linearity is very much smaller than the errors we have for the QSO $\bar{\xi}$. At smaller scales we may be able to extrapolate the biasing model and use the non-linear evolution of $\bar{\xi}$ (Hamilton et al. 1991), but to use the linear biasing process at smaller scales we have to make very large assumptions about the mechanism of biasing, particularly when we reach scales of a few Mpc, corresponding to the scale of galaxy clusters. We can obtain a much less model dependent result if we use linear theory. Linear theory predictions can also be made in a general case with any value of $\Omega_\circ$, so instead of $(1+z)$ we have a general growth $G(z,\Omega_\circ)$,

$$b_{q\rho}=\left[\frac{\xi_{qq}(z)}{\xi_{gg}(0)}\right]^{1/2}b_{g\rho}-\frac{1}{G(z,\Omega_\circ)}+1 \qquad (17)$$

In Fig. 9(a) we show how the predicted $\bar{\xi}(10)$ (based on the measured $\bar{\xi}(10)$ at $z=1.27$) at $z=0$ varies as a function of $b_{g\rho}$ and $\Omega_\circ$, each result will correspond to a value of $b_{q\rho}$. In Table 2 we show the values calculated for the $b_{q\rho}(z=0)$, $\bar{\xi}_{qq}(10,z=0)$ and $r_\circ(z=0)$ for $b_{g\rho}=1$ and 2 and various $\Omega_\circ$. With $\Omega_\circ=1$ and $b_{g\rho}=1$ we find $b_{q\rho}=1.47\pm0.16$ but with $b_{g\rho}=2$ this increases to $b_{q\rho}=2.38\pm0.32$. These correspond to $\bar{\xi}(10)=2.16\pm0.47$ and 1.42 ± 0.38 respectively at $z=0$. If we consider higher biasing of galaxies (that is, a lower effective mass correlation function) or low $\Omega_\circ$ then the amplitude of $\bar{\xi}(r)$ is reduced. So for our biasing model the clustering amplitude of QSOs at the present is a maximum when $\Omega_\circ = 1$ and $b_{g\rho} = 1$. Taking these parameters and assuming a -1.8 power law, we obtain a scale length $r_\circ(z=0) = 9.23 \pm 1.11\ h^{-1}$ Mpc. This value is obviously significantly smaller than the value of $18 \pm 2\ h^{-1}$ Mpc discussed above (Mo & Fang 1993) without taking into account biasing. We find that the QSO amplitude lies close to that of the galaxies for all but the $\Omega_\circ = 1$, $b_{g\rho} = 1$ case, and in all cases is significantly lower that the clustering amplitude associated with galaxy clusters, eg. $r_\circ = 14.3 \pm 2.35\ h^{-1}$ Mpc (2σ errors), (Dalton et al. 1994).

Now considering the low redshift Seyfert result (Paper II), we find that a model where clustering is stable in comoving coordinates is inconsistent with the case of $\Omega_\circ = 1$ and $b_{g\rho} = 1$ (Fig. 9(b)). With the assumption that AGN at both high and low redshift belong to the same population we can reject certain combinations of $\Omega_\circ$ and $b_{g\rho}$. The low redshift clustering amplitude for a combination of the IRAS Seyferts (Paper II) and EMSS QSOs (Boyle & Mo 1993) is $\bar{\xi}(10) = 0.50 \pm 0.31$. The $\Omega_\circ = 1$, $b_{g\rho} = 1$ model above gives $\bar{\xi}(10) = 2.16 \pm 0.47$ for high z QSOs evolved to the present day and these two values are inconsistent at the 2.9σ level. This then can be interpreted as a rejection of the $\Omega_\circ = 1$, $b_{g\rho} = 1$ scenario. In a similar manner the $\Omega_\circ = 1$, $b_{g\rho} = 2$ is only rejected at the 1.9σ level as the predicted QSO amplitude at $z = 0$ is lower. For $\Omega_\circ = 0.1$ and $b_{g\rho} = 1$ the present day QSO clustering is estimated to be $\bar{\xi}(10) = 1.62 \pm 0.57$ which is only inconsistent with the low z clustering at the 1.7σ level (note that the errors are larger on the low $\Omega_\circ$ estimates as we find less pairs of QSOs within 10 h^{-1} Mpc). Thus we find that the slow evolution of QSO clustering is consistent to better than 2σ with either $\Omega_\circ = 1$, $b_{g\rho} = 2$ or $\Omega_\circ = 0.1$, $b_{g\rho} = 1$.

7 QSO CLUSTERING AND CMB NORMALIZED CDM

Using the combined sample we next compare the QSO correlation function to the amplitude of CMB fluctuations from *COBE*, using parametric models of the mass correlation function to extrapolate from *COBE* scales to the region between 8 and 50 h^{-1} Mpc. In particular we use the Fourier transform of the generic CDM power spectrum (Efstathiou, Bond & White 1992) which is a good fit to a wide range of cosmologies in the linear regime,

$$P(k) = \frac{Bk}{\{1 + [ak + (bk)^{3/2} + (ck)^2]^\nu\}^{2/\nu}} \tag{18}$$

where $a = (6.4/\Gamma)\ h^{-1}$ Mpc, $b = (3.0/\Gamma)\ h^{-1}$ Mpc, $c = (1.7/\Gamma)\ h^{-1}$ Mpc, and $\nu = 1.13$. The shape parameter $\Gamma \simeq \Omega_\circ h$ for $\Omega_\circ = 1$ CDM and flat CDM with a non-zero cosmological constant. The amplitude of the power spectrum, B, is normalized to the *COBE* two year quadrupole, $Q_{\rm rms} = 17.6 \pm 1.5\mu$K (Bennett et al. 1994). To convert this value to the power spectrum amplitude, B, we use the fact that the coefficients for the spherical harmonic expansion of the temperature fluctuations of the CMB are given by,

$$\langle |a_l^m|^2 \rangle = 4\pi^2 \left(\frac{H_\circ}{c}\right)^4 \left(\frac{\Omega_\circ}{D_\circ}\right)^2 \int_0^\infty P(k) j_l^2(kr) \frac{dk}{k^2} \tag{19}$$

(Peebles 1993), where $P(k)$ is the present day power spectrum (see above), j_l is the spherical Bessel function of order l, r is the angular size distance defined in equation (4) and $D_\circ$ is the growth rate of mass perturbations normalized to an Einstein-de Sitter universe at $z = 0$. We are comparing the CDM models to QSOs with a mean redshift of $z = 1.27$ so we replace the $D_\circ$ with $D(z = 1.27)$. D is a function of z and $\Omega_\circ$ and is described by

$$D = \left(\frac{x}{x_\circ}\right)(x^3 + 1)^{1/2} \int_0^1 \frac{dy}{(1 + x^3 y^{6/5})^{3/2}} \tag{20}$$

$$x = \frac{(\Omega_\circ^{-1} - 1)^{1/3}}{1 + z} \tag{21}$$

for a universe with zero curvature (Peebles 1984) (for other cosmologies this is given in Peebles (1980)). If we now assume a scale invariant spectrum on *COBE* scales, that is $P(k) = Bk$, and use

$$Q_{\rm rms} = \left(\frac{5C_2}{4\pi}\right)^{1/2} T_\circ \tag{22}$$

where $C_2 = \langle |a_2^m|^2 \rangle$ and $T_\circ = 2.735 \pm 0.006$K (Mather et al. 1990), we can then obtain,

$$B = \left(\frac{Q_{\rm rms}}{T_\circ}\right)^2 \frac{12}{5\pi} \left(\frac{c}{H_\circ}\right)^4 \left(\frac{D}{\Omega_\circ}\right)^2 \tag{23}$$

Once the power spectrum is normalized it is a simple process to produce a corresponding $\xi(r)$, via

$$\xi(r) = 4\pi \int_0^\infty k^2 P(k) \frac{\sin(kr)}{kr} dk \tag{24}$$

To fit the above models for ξ to the QSO data we now have two effectively free parameters, Γ (shape of $P(k)$) and $b_{q\rho}$, the bias of the QSOs at $z = 0$. The amplitude of $P(k)$ and hence $\xi(r)$ is normalized to the CMB results of *COBE*, to obtain $\xi(z = 1.27)$ we have to assume some form of evolution which depends on $\Omega_\circ$, below we will look at two cases, one assuming $\Omega_\circ = 1.0$, the second assuming $\Omega_\circ = 0.2$. Taking the *COBE* normalizations we cover the likely parameter space in Γ and $b_{q\rho}$, fitting the models to the QSO ξ on scales ~ 8 to 50 h^{-1} Mpc. In all cases we fit to the QSO data with the CFHT 'supercluster' removed as this would add excess power at $\sim 30\ h^{-1}$ Mpc scales.

In the case of $\Omega_\circ = 1$, $\Gamma \sim h$. Fig. 10(a) shows the confidence contours for this fit to the QSO ξ. Within this parameter space it is clear that we cannot, with present statistics, constrain both the amplitude and shape of the linear correlation function if we let both vary freely within the plane. If we constrain Γ to a particular value then we can obtain a statistically significant result for the bias. Taking the value for standard CDM ($\Gamma = 0.5$), then best value of the present day QSO bias is $1.40^{+0.28}_{-0.43}$ and the 3σ upper limit is 1.93.

We can carry out the same analysis with a different cosmology. In Fig. 10(b) we plot the confidence contours and best fit for the case of $\Omega_\circ = 0.2$ and $\lambda_\circ = 0.8$ (ΛCDM), here Γ only varies from $0 - 0.4$ (as $\Gamma = 0.2h$). Here again we see that without firstly constraining one of the two parameters the range of possible values for both parameters is not well constrained. A currently popular scenario is CDM with $\Gamma = 0.2$ and a cosmological constant ($\lambda_\circ \simeq 0.8$). Assuming this model we obtain $b_{q\rho}(z = 0) = 1.2^{+0.13}_{-0.18}$ and a 3σ upper limit of 1.53. In Section 8 we will compare this result and the evolution result of Section 6.

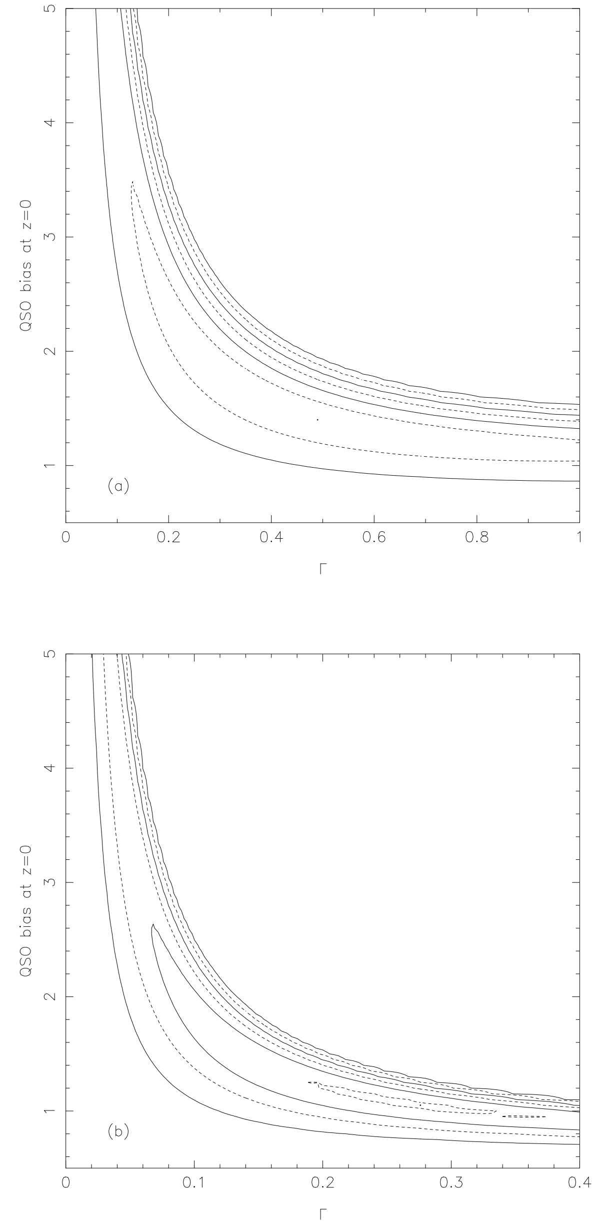

Figure 10. Confidence levels for fits of the combined QSO ξ to CDM type correlation functions with free parameters Γ and $b_{q\rho}$ for (a) $\Omega_\circ = 1$, and (b) $\Omega_\circ = 0.2$, $\lambda_\circ = 0.8$. dotted lines are 0.5σ intervals, solid lines are 1σ intervals.

8 DISCUSSION

8.1 Small scale clustering

Assuming a -1.8 power law the value of $\bar{\xi}(10)$ implies $r_\circ = 5.4 \pm 1.1\ h^{-1}$ Mpc which is fully consistent with the present day galaxy value. This also agrees with the value found by Mo & Fang (1993) of $r_\circ = 6.6 \pm 0.5\ h^{-1}$ Mpc, but is lower than the Andreani & Cristiani (1992) value of $r_\circ \sim 10\ h^{-1}$ Mpc. It is not clear why this last result is higher, however the statistics for QSO clustering are still not very good, and future surveys are likely to clear up many outstanding problems. Andreani & Cristiani also find little evidence for evolution of clustering in comoving coordinates, consistent with the slow evolution we describe below.

The natural conclusion of assuming that Seyferts and QSOs come from an equally clustered population is that their clustering does not evolve in comoving coordinates, and has an amplitude of $r_\circ \sim 6.0\ h^{-1}$ Mpc (Paper I). This suggests that QSOs randomly sample a comoving galaxy distribution on scales $\sim 10\ h^{-1}$ Mpc. Recent results from the cross-correlation of low redshift EMSS QSOs with APM galaxies (Smith, Boyle & Maddox 1995) where the cross-correlation amplitude is found to be similar to the galaxy auto-correlation amplitude also support the idea that QSOs randomly sample galaxies.

We construct a biasing model to further test the clustering evolution of QSOs. This model gives an upper limit to the present day clustering of QSOs of $r_\circ(z = 0) = 9.23 \pm 1.11\ h^{-1}$ Mpc. When we postulate that the low redshift Seyferts and the high redshift QSOs are clustered in the same way we obtain a strong constraint on the evolution of clustering and hence on a combination of biasing and $\Omega_\circ$. We find that the $\Omega_\circ = 1$, $b_{g\rho} = 1$ scenario is ruled out at almost the 3σ level. $\Omega_\circ = 1$, $b_{g\rho} = 2$ and $\Omega_\circ = 0.1$, $b_{g\rho} = 1$ are consistent to better than 2σ with the QSO evolution. When we take a very low $\Omega_\circ$ ($\simeq 0.02$) we find consistency to $\sim 1\sigma$. Thus the evolution of QSO clustering over this redshift range seems to imply a low value of $\Omega_\circ$ or a strongly biased galaxy distribution (and therefore a biased QSO distribution).

8.2 Intermediate scale clustering

We next compared the QSO ξ to one produced via a Fourier transform of the generic CDM power spectrum (Efstathiou et al. 1992) normalized to the CMB results from the two-year *COBE* data (Bennett et al. 1994). Because the shape of our correlation function is not well constrained we are effectively comparing the QSO clustering amplitude to the CMB anisotropy amplitude using a model power spectrum to extrapolate from *COBE* to scales where we have a QSO clustering signal ($\sim 8 - 50\ h^{-1}$ Mpc). In the case of standard CDM ($\Omega_\circ = 1$, $\Gamma = 0.5$) the QSO biasing at the present day is strongly constrained and has a 3σ upper limit of 1.93. Similarly when we assume CDM plus a cosmological constant ($\Omega_\circ = 0.2$, $\lambda_\circ = 0.8$, $\Gamma = 0.2$) the 3σ upper limit on QSO biasing is 1.53. For $\Omega_\circ = 1$ and $\Gamma = 0.5$ the best fit is $b_{q\rho}(z = 0) = 1.40^{+0.28}_{-0.43}$; for $\Omega_\circ = 0.2$, $\lambda_\circ = 0.8$ and $\Gamma = 0.2$ this is $1.20^{+0.13}_{-0.18}$. We can use our biasing model of Section 6 to imply a present day clustering amplitude from these values, we find $\bar{\xi}(10, z = 0) = 2.30^{+1.87}_{-1.22}$ and $\bar{\xi}(10, z = 0) = 3.54^{+2.80}_{-2.46}$ for standard CDM and ΛCDM respectively. We can compare this to the low redshift AGN clustering result ($\bar{\xi}(10, z \simeq 0) = 0.50 \pm 0.31$). Although both the estimates are larger than those found in Section 6, the increased errors result in no significant inconsistency with the low redshift clustering.

Thus the fits to the intermediate scale QSO correlation function (at $z = 1.27$) prefer a low bias for $\Omega_\circ = 1$ CDM with $\Gamma \leq 0.5$. This is in contrast to the small scale evolution results of Section 6 where a high bias is required for the $\Omega_\circ = 1$ case. Although the errors are still large, there exists a narrow range where the two bias estimators overlap. For ΛCDM we find a similar result, which also suggests fast evolution of clustering, again in contradiction (although not significantly) to the small scale evolution results. With increased statistics it may, in the future, be possible to rule out these two CDM models from the small scale evolution of the QSO clustering.

8.3 Large scale clustering

The addition of the LBQS survey to the samples used in Paper I greatly increases our statistics at large scales, the number of pairs per bin in the LBQS becomes greater than in the Durham/AAT sample at scales $> 100\ h^{-1}$ Mpc. On these scales the combined sample has errors of ± 0.025. We can compare this to previous estimates, for example, $\pm 0.1 - 0.15$ for a sample of 125 QSOs at $1.5 < z < 3.0$ (Osmer & Hewett 1991).

When we look at the region at $40 - 100\ h^{-1}$ Mpc where an anti-correlation was seen in the Durham/AAT sample, we find that the LBQS (similar to the CFHT and ESO/AAT) shows no sign of this signal on these scales. The Durham/AAT is still found to be negative in this region, in particular at $\simeq 89\ h^{-1}$ Mpc. A direct comparison between the LBQS and Durham/AAT samples produces a 2σ inconsistency at scales $40 - 100\ h^{-1}$ Mpc.

A combined sample of all surveys for $0.3 < z < 2.2$ gives us a ξ which is to first order consistent with a Poisson distribution on all scale larger than $40\ h^{-1}$ Mpc. There is a marginal signal at $\sim 100\ h^{-1}$ Mpc which could be tested by larger samples.

If we change our assumed cosmology then we see some change in the correlation function. For $q_\circ = 0.01$ we find that the negative region at $\simeq 89\ h^{-1}$ Mpc has now moved out past $100\ h^{-1}$ Mpc and similarly for the low $\Omega_\circ$ inflationary Λ case ($k = 0$), this moves to $\sim 200\ h^{-1}$ Mpc. The Λ model, if incorrect, should be rejected by the change of scale of linear features in the correlation function. We see negative regions in the correlation function for this cosmology in both low and high redshift bins, and these features don't correspond to the same scale. However to conclude that these features have the same source and therefore reject the Λ cosmology is difficult considering the statistical significance of these signals.

We test the Λ model by comparing $\bar{\xi}(25)$ for this model to a -1.8 power law with $r_\circ = 6\ h^{-1}$ Mpc, we find a 2.9σ inconsistency. In this cosmology the linear growth rate from $z = 1.27$ to $z = 0.0$ is low, only a factor of 1.26, compared to 2.27 for $\Omega_\circ = 1$. We therefore have evolution which is approximately stable in comoving coordinates. If low redshift AGN and high redshift QSOs sample the same population this result can be used to reject the Λ model. With larger samples it will be possible to further constrain the value of Λ.

9 CONCLUSIONS

We have analysed a total sample of > 1500 QSOs with $0.3 < z < 2.2$. In particular we have looked at the clustering in the LBQS survey and used a simple but self consistent model for biased clustering evolution. From our analysis we draw the following conclusions:

1. At small scales we find a marginal detection of clustering in the LBQS; assuming $\Omega_\circ = 1$ we find $\bar{\xi}(10) = 1.86 \pm 1.28$. With $\Omega_\circ = 0.1, 0.02$ and cases with cosmological constants there is no significant clustering at this scale in the LBQS. When we combine this with other samples we find $\bar{\xi}(10) = 0.83 \pm 0.29$ for $\Omega_\circ = 1$ (including re-analysed CFHT and ESO/AAT data). The results for other cosmologies are shown in Table 1. The LBQS is not an efficient sample to use for clustering at this scale due to it's sparsely sampled nature.

2. At large scales the LBQS makes a significant contribution to clustering statistics. We find that the LBQS does not support the anti-correlation found in the Durham/AAT survey at scales $40 - 100\ h^{-1}$ Mpc (Paper I) at the 2σ level, and find no signal of this nature in the LBQS. At $> 100\ h^{-1}$ Mpc the upper limits on a detected signal is now at the ± 0.025 level.

3. Using a model for biased clustering evolution based on the peaks-bias formalism (Bardeen et al. 1986) we derive a present day clustering amplitude for QSOs. In the case of $\Omega_\circ = 1$ with an unbiased galaxy distribution we find $\bar{\xi}(10) = 2.16 \pm 0.47$. Assuming a -1.8 power law this is equivalent to $r_\circ = 9.23 \pm 1.11$. If we decrease $\Omega_\circ$ or increase the galaxy biasing then this value will decrease. Hence this value of $r_\circ$ is an upper limit on the present day QSO clustering amplitude. This value is significantly lower than the clustering amplitude of rich galaxy clusters.

4. If the low redshift AGN population and the high redshift QSO population are both clustered in the same way then the clustering evolution is best fit by a slowly evolving model. The above $\Omega_\circ = 1$, unbiased galaxies, model is then inconsistent with the clustering evolution at the $\sim 3\sigma$ level. The slow development of QSO clustering therefore implies low $\Omega_\circ$ and/or high biasing.

5. We compare the QSO ξ to linear theoretical predictions of CDM correlation functions, normalized to the CMB anisotropy (Bennett et al. 1994). With two free parameters (biasing and Γ) we cannot obtain a significant result. If we assume a value of Γ then we can obtain a constraint on the bias of QSOs. For $\Omega_\circ = 1$, $\Gamma = 0.5$ (standard CDM) we find $b_{q\rho}(z = 0) = 1.40^{+0.28}_{-0.43}$. For $\Omega_\circ = 0.2$, $\lambda_\circ = 0.8$, $\Gamma = 0.2$ (ΛCDM) the value found is $1.20^{+0.13}_{-0.18}$.

6. For a flat cosmology with $\lambda_\circ = 0.97$, $\Omega_\circ = 0.03$ we find an amplitude at $25\ h^{-1}$ Mpc of $\bar{\xi}(25) = 0.74 \pm 0.23$, this is inconsistent with $\xi = (r/6)^{-1.8}$ at the 2.9σ level, confirming the result obtained in Paper I. If we assume that high redshift QSOs and low redshift AGN belong to the same population then this is a significant rejection of the inflationary $\Lambda > 0$ cosmology.

7. The small scale evolution and intermediate scale comparisons to the CMB (via CDM) imply a narrow range of acceptable values for the bias in $\Omega_\circ = 1$ CDM around $b_{q\rho} \simeq b_{g\rho} \simeq 2$ and similar, if not lower, values for ΛCDM. With the advent of new QSO samples with order of magnitude improvements in numbers a combination of small scale evolution and comparison to the CMB will give us a great opportunity to independently discriminate between different values of biasing and $\Omega_\circ$.

ACKNOWLEDGMENTS

SMC acknowledges the support of a Durham University Research Studentship. We thank P.C. Hewett for providing LBQS data and for many useful comments.

REFERENCES

Andreani P., Cristiani S., 1992, ApJ, 398, L13
Bardeen J.M., Bond J.R., Kaiser N., Szalay A.S., 1986, ApJ, 304, 15
Barrow J.D., Bhavsar S.P., Sonoda D.H, 1984, MNRAS, 210, 19P
Bennett C.L. et al., 1994, ApJ, 436, 423
Broadhurst T.J., Ellis R.S., Koo D.C, Szalay A.S., 1990, Nature, 343, 726
Boyle B.J., 1986, PhD Thesis, University of Durham
Boyle B.J., Fong R., Shanks T., Peterson B.A., 1990, MNRAS, 243, 1
Boyle B.J., Jones L.R., Shanks T., 1991, MNRAS, 251, 482
Boyle B.J., Couch W.J., 1993, MNRAS, 264, 604
Boyle B.J., Mo H.J., 1993, MNRAS , 260, 925
Crampton D., Schade D., Cowley A.P., 1985, AJ, 90, 987
Crampton D., Cowley A.P., Hartwick F.D.A., 1987, ApJ, 314, 129
Crampton D., Cowley A.P., Hartwick F.D.A., 1989, ApJ, 345, 59
Croom S.M., Shanks T., Boyle B.J., 1995, in Maddox S.J., Aragon-Salamanca, A., eds, Wide-Field Spectroscopy and the Distant Universe (35th Herstmonceux Conf.)
Dalton G.B., Croft R.A.C., Efstathiou G., Sutherland W.J., Maddox S.J., Davis M., 1994, MNRAS, 271, L47
de Grijp M.H.K., Miley B.K., Lub J., 1987, AASup, 70, 95
Efstathiou G., Rees M.J., 1988, MNRAS, 230, 5P
Efstathiou G., Bond J.R., White S.D.M., 1992, MNRAS, 258, 1P
Ellingson E., Yee H.K.C., Green R.F., ApJ, 371, 49
Foltz C.B., Chaffee F.H., Hewett P.C., MacAlpine G.M., Turnshek D.A., Weymann R.J., Anderson S.F., 1987, AJ, 94, 1423
Georgantopoulos I., Shanks T., 1994, MNRAS, 271, 773
Hamilton A.J.S., Kumar P., Lu E., Matthews A., 1991, ApJ, 374, L1
Hewett P.C., Foltz C.B., Chaffee F.H, 1993, ApJ, 406, L43
Hewett P.C., Foltz C.B., Chaffee F.H, 1995, AJ, 109, 1498
Hintzen P., Romanishin W., Valdes F., 1991, ApJ, 366, 7
Loveday J., Maddox S.J., Efstathiou G., Peterson B.A., 1995, ApJ, 442, 457
Mather J.C. et al., 1990, ApJ, 354, L37
Mo H.J., Jing Y.P., Borner G., 1992, ApJ, 392, 452
Mo H.J., Fang L.Z., 1993, ApJ, 410, 493
Osmer P.S., 1981, ApJ, 247, 762
Osmer P.S., Hewett, P.C., 1991, ApJS, 75, 273
Park C., Vogeley M.S., Geller M.J., Huchra J.P., 1994, ApJ, 431, 569
Peebles P.J.E., 1980, The large-Scale Structure of the Universe. Princeton Univ. Press, Princeton, NJ
Peebles P.J.E., 1984, ApJ, 284, 439
Peebles P.J.E., 1993, Principles of Physical Cosmology, Princeton, New Jersey
Refsdal S., 1966, MNRAS, 132, 101
Shanks T., Fong R., Boyle B.J., Peterson B.A., 1987, MNRAS, 227, 739
Shanks T., Boyle B.J., 1994, MNRAS, 271, 753
Smith R.J., Boyle B.J., Maddox S.J., 1995, MNRAS in press
Yee H.K.C., Green R.F., 1987, ApJ, 319, 28
Zitelli V., Mignoli M., Zamorani G., Marano B., Boyle B.J., 1992, MNRAS, 260, 925